Environmental Science and Pollution Research (2021) 28:65610–65620
https://doi.org/10.1007/s11356-021-15487-w

RESEARCH ARTICLE

Performance analysis of crushed gravel sand heat storage and biomass evaporator-assisted single slope solar still

Ramasamy Dhivagar[1,2] · Murugesan Mohanraj[1,3] · Yerzhan Belyayev[3,4]

Received: 21 March 2021 / Accepted: 13 July 2021 / Published online: 28 July 2021

Abstract

In this research work, the productivity, energy, exergy, and economic and enviro-economic performance in crushed gravel sand heat storage and biomass evaporator-assisted solar still (CGS-BSS) have been investigated and compared the results with conventional solar still (CSS) under the similar climatic conditions of Coimbatore City during the year 2019. The heat accumulated in crushed gravel sand and biomass evaporator have been used to preheat the inlet saline water and air vapor before entering into the solar still. This results in enhanced air vapor mixture temperature and evaporative heat transfer rate of CGS-BSS significantly. The productivity, energy, and exergy efficiencies in CGS-BSS were improved by 34.6%, 34.4%, and 35%, respectively when compared to CSS. In economic analysis, the payback period (PBP) in both CGS-BSS and CSS was estimated to be about 4.7 months and 3.9 months, respectively. Furthermore, in enviro-economic analysis, the CO_2 emission estimated in CGS-BSS and CSS was about 16.63 tons and 8.18 tons, respectively during its lifetime of 10 years.

Keywords Biomass evaporator · Crushed gravel sand · Energy · Exergy · Productivity · Solar still

Introduction

In present scenario, the ratio of pure water is limited due to population density and globalization. Even though the large quantity of water is available in oceans, it is not used significantly by humans for their daily needs. On other side, the available pure water in rivers and lakes are infected by industrial wastes considerably. Hence, it is very difficult to provide pure water in remote and arid areas. In order to overcome this shortage, it is essential to identify the suitable method to covert the waste water into useful pure water effectively and economically. Solar desalination is a very simple method to enhance the ratio of pure water. In this technique, the required quantity of purified water is obtained by condensing the water vapor in solar still. The construction of solar still is easy, and low cost is required due to free solar energy. Desalination using solar still method has no harmful impact to the environment and handling technique is simple.

In order to improve the solar still performance, several heat storage materials have been used in solar still basin by many researchers. The outcomes proved that the productivity was significantly improved by heat storage materials like fins, nanoparticles, stones, jute cloths, and PCM. Rabhi et al. (2017) improved the solar still surface area using pin-fin absorber and observed enhanced productivity of about 14.5% significantly. In addition, they have used condenser in solar still which results in enhanced productivity of about 32% when compared to CSS. Sharshir et al. (2018) used copper oxide and graphite nanoparticles in the absorber plate of solar still to improve the daily productivity and compared the results with CSS. The results proved that, the enhanced productivity of about 41% and 32%, respectively observed for the copper oxide and graphite nanoparticles, respectively. Dumka et al. (2019a) used cotton bags filled with sand in the absorber plate of solar still to enhance the productivity during summer climate conditions of India. The experiments have been

Responsible Editor: Philippe Garrigues

✉ Ramasamy Dhivagar
dhivagar.papers@gmail.com

1 Department of Mechanical Engineering, Hindusthan College of Engineering and Technology, Coimbatore 641032, India

2 Department of Mechanical Engineering, QIS College of Engineering and Technology, Ongole 523272, India

3 Department of Mechanics, Al-Farabi Kazakh National University, Almaty, Kazakhstan

4 Department of Applied Mechanics and Engineering Graphics, Satbayev University, Almaty, Kazakhstan

conducted with different mass of sand and compared the outcomes with CSS. The results observed that the solar still thermal efficiency was enhanced to 31.3 (40 kg) and 28.9% (50 kg), respectively. The results also proved that the higher quantity of sand availability in basin of solar still has lowered the productivity considerably. Modi and Modi (2019) found the significant improvement in solar still performance when the jute and cotton cloths were used in basin. The outcomes observed in jute cloth solar still were considerably higher than the results observed in the usage of cotton cloth. The observed results proved that, the productivity was enhanced in jute cloth solar still by 18% (1 cm water depth) and 24.5% (2 cm water depth), respectively when the results compared with cotton cloth solar still. In addition, the basin saline water depth has significant role to heighten the productivity. Omara et al. (2020) used different PCM in two solar stills (passive and active type) and assessed the productivity during sunny days. The observed outcome proved that the passive and active solar still have the productivity improvement of about 120% and 700%, respectively, under nocturnal observations. The results also observed that the paraffin wax has been widely used in many research works. Even though many researchers have used this material, it has poor thermal conductivity when compared to other heat storage materials (Dhivagar and Sundararaj 2018). Chandran et al. (2020) improved the daily productivity of biomass-assisted stepped cup solar still and simple stepped cup solar still by 70% and 12%, respectively, when compared to CSS. The results also proved that the overall evaporative heat transfer rate was significantly improved by biomass heat source.

In solar stills, the productivity rate has been significantly heightened by integrating with external heat sources like solar water heaters, air heaters, and heat pumps. Omara et al. (2013) evaluated the productivity improvements in solar water heater-assisted wick-type solar still and compared the results using CSS. The results observed that the proposed model enhanced the daily productivity by 114% during peak sunshine hours. Kabeel et al. (2016) used preheating technique to enhance the hourly productivity by solar air heater-assisted solar still. The inlet air was preheated using heater and passed into the solar still to enhance the evaporation process. The outcomes proved that the productivity was significantly enhanced by 9.4 kg/m^2 when compared to CSS. In addition, the evaporation rate was mainly influenced by the inlet air and saline water temperature. Belyayev et al. (2019) numerically evaluated the productivity performance of heat pump-assisted solar still using PCM under the climate conditions of Kazakhstan. The outcomes proved that, the productivity and energy efficiency were improved by 80% and 64%, respectively when compared to CSS.

Many researchers have concentrated to evaluate the energy and exergy performance of solar stills. Sakthivel and Arjunan (2019) evaluated the energy and exergy efficiencies of cotton cloth solar still during summer climate conditions in India. The results observed that the use of 6 mm thickness in basin was enhanced energy and exergy efficiencies by 23.8% and 2.6%, respectively. In addition, the improved productivity of about 24.1% was observed when compared to CSS. The results also proved that the usage of cotton cloth materials with different thickness in solar still basin significantly enhanced the energy and exergy performance. Hassan (2019) investigated the energy and exergy analysis in parabolic trough collector-assisted solar still during sunny days. The outcomes observed that the saline water temperature of 73 °C enhanced the hourly productivity significantly. In addition, the energy and exergy efficiencies were increased to 49.9% and 2.6%, respectively, when compared with CSS. Dhivagar and Sundararaj (2019) used preheating technique in coarse aggregate-assisted solar still and increased the energy and exergy efficiencies to 28% and 5.5%, respectively, when compared to CSS. Dubey and Mishra (2020) estimated the productivity improvement in solar still using ferrite ring magnets and GI sheet by 21.7% effectively. The results also observed that the energy and exergy efficiencies were significantly increased to 31.3% and 22.6%, respectively. In addition, the usage of magnets in the absorber plate improved the daily productivity considerably.

Recently, several research works have been concentrating on the solar still performance in economically and enviro-economically aspects. Senthil Rajan et al. (2014) improved the daily productivity of biomass heat source-assisted solar still by 73% when compared to CSS. The outcomes have been observed in this model by response surface methodology (RSM). The results also observed that the PBP was estimated as 126 days and 480 days, respectively, for continuous flow and solar modes. Sharon et al. (2017) compared the tilted solar still performance with wick-type solar still and proved that the productivity of tilted solar still was improved by 19.7% under the climate conditions of India. The titled solar still has improved energy and exergy efficiencies by 41% and 3%, respectively, when compared to wick type. In addition, the PBP and CO_2 emission of titled solar still were estimated as 2.8 years and 17.65 tons, respectively, during the lifetime of 20 years. Bait (2019) evaluated the performance of solar collector-assisted tubular solar still during sunny days in Algeria. The results observed that the annual productivity was increased to 549.7 kg/m^2 which is 26.3% lower than CSS. The results also observed that the hourly and global exergy efficiency was improved by 7% and 30% when compared to CSS. The PBP and CO_2 emission for this proposed model was estimated to be about 21 years and 4.42 tons, respectively. Dhivagar et al. (2020) evaluated the energy and exergy efficiencies in coarse aggregate-assisted solar still by 32% and 4.7%, respectively, during the summer climate conditions of Coimbatore. The results observed that the PBP and CO_2 emission were estimated as 4.3 months and 8.27 tons at

1-cm water depth. During experimentation, the minimal saline water depth in solar still basin was significantly increasing the productivity as well as thermal performance (Abdullah et al. 2020).

The above literature showed that several heat storage/retain techniques were used in solar still basin internally and externally to improve the overall performance. However, there is no experimentation carried out using crushed gravel sand heat storage and biomass evaporator in solar still to preheat the inlet saline water and air vapor. Hence, the heat accumulated in crushed gravel sand and biomass evaporator is used in solar still to enhance the daily productivity. Furthermore, the energy and exergy efficiencies in CGS-BSS are compared with CSS to evaluate the energy conversion and losses. Finally, the cost effectiveness and CO_2 emissions of both CGS-BSS and CSS are estimated using economic and enviro-economic analyses.

Experiments

The experimentation and its procedure followed in CGS-BSS are discussed in this section. To compare the observations, the required experimentation is conducted in CSS separately during the same day.

Experimental setup

The schematic and photographic view of CGS-BSS is depicted in Figs. 1 and 2. In this, the solar still basin area is 0.65 m × 0.78 m, and the capacity of water supply tank is 50 l. The solar still basin and its wall are fabricated by mild steel (thick 1.2mm). To enhance the heat absorption rate in basin, the black coating is recommended at peak sunshine hours. The glass cover (thick 3 mm) is placed with titled angle of 12° at the top of the solar still. The entire system is closed completely using silicon rubber to prevent vapor losses to the atmosphere. The outside walls are covered using thermocol (thick 25 mm) to retain the heat during low sunshine hours. The temperature at various portions of solar still is measured by thermocouples, and it is connected using temperature indicator. A drain channel was placed at the bottom of solar still to collect the condensate. To enhance the solar irradiation absorption rate in glass cover, the solar still is kept along east-west direction by facing towards the south direction (Dhivagar et al. 2021a). The thermal properties of various sands are listed in Table 1. From this, crushed gravel sand is selected by its higher thermal conductivity and specific heat capacity. Finally, around 60 kg of crushed gravel sand (bed thick 8.5 cm) is used for the preheating technique.

The biomass tank is made using tin container with the dimension of 250×250×750 mm. The shell thickness of the biomass tank is 10 mm. The lower biomass feed section is filled with 20 kg of cow dung and is connected to the biogas collector. The upper evaporator section is coupled with the pipe in which the hot vapor passes into the solar still. Also, the water circulation tube is made of copper with 0.5 mm thickness and 860 mm length, respectively. This tube acts as heat transfer pipe from crushed gravel sand to saline water. The saline water and hot air vapor are controlled using ball valves in both solar still and evaporator. The basin saline water depth (1 cm) is observed at 1-h interval and maintained consistently. The salt deposition in the basin was cleaned periodically. The measuring device specifications are listed in Table 2.

Experimental procedure

In this experimentation, the heat accumulated in crushed gravel sand and biomass evaporator ;is used for the preheating techniques. The required quantity (1 kg) of inlet saline water is heated using crushed graved sand before enter into the solar still basin. Further, 2 kg of saline water is filled in the biomass evaporator and the biomass tank is ignited manually using locally available materials. The heat generated inside the biomass tank is absorbed by the evaporator to heat the saline water. Finally, the produced hot vapor is sent to the inlet of the solar still using an evaporator pipe to enhance the heat transfer process. This results in improved the evaporation process significantly due to the preheated saline water using crushed gravel sand and hot air vapor from biomass evaporator. The biogas generated in biomass tank is collected separately.

The provided experimental observation has been made on 05.02.2019 when the minimum fluctuations were observed in ambient conditions. Before the experimentation, the dust accumulated over the glass cover was cleaned by soft cloth. This leads to affect the heat absorption and productivity of the solar stills (Dhivagar et al. 2021b). During the experimental observations, the solar irradiation, ambient temperature, ambient wind velocity, crushed gravel sand temperature, feed water (inlet saline water) temperature, air vapor mixture temperature, saline water temperature and productivity were measured at every 1-h interval from 9:00 hours to 21:00 hours. In CSS, the experimental observation has been made from 9:00 hours to 19.00 hours due to availability of solar irradiation. In CGS-BSS and CSS, 20-day experimental trials have been made to check the transient behavior, consistency of the readings and errors. Finally, the observed experimental data were used for overall performance comparison.

Energy analysis

The performance of energy conversion is evaluated using first law of thermodynamics. The required mathematical relations are provided with assumptions (Elango et al. 2015):

- Inclination angle of glass cover is negligible.
- The saline water depth is maintained constant.

Table 1 Thermal properties of various sands

Sands	Properties		
	Thermal conductivity (W/m/K)	Specific heat capacity (kJ/kg·K)	Water absorption rate (%)
Sandy clay	1.61	1.696	26.5
Fine sand	2.75	1.632	24.6
Brown sandy clay	3.2	1.104	9
Crushed gravel sand	3.57	1.764	24.5

- The water vapor leakages from solar stills are negligible.
- The thermo-physical properties of glass cover and saline water are assumed constant.

Convective heat transfer coefficient (Elango et al. 2015):

$$h_{c,\ w-g} = 0.884\left[T_w - T_g + \frac{(P_w - P_g)\ T_w + 273}{268,900 - P_w}\right]^{1/3} \quad (1)$$

Evaporative heat transfer coefficient (Elango et al. 2015):

$$h_{eva\quad w-g} = 0.016\ h_{c\quad w-g}\frac{(P_w - P_g)}{(T_w - T_g)} \quad (2)$$

Radiative heat transfer coefficient (Elango et al. 2015):

$$h_{r,\ w-g} = \sigma\varepsilon_{eff}\left[(T_w + 273)^2 - (T_g + 273)^2\right](T_w + T_g + 546) \quad (3)$$

Latent heat of vaporization (Elango et al. 2015):

$$L = 2.4935 \times 10^6 \times \left[1 - 9.4779 \times 10^{-4}\ T_w + 1.3132 \times 10^{-7} \times T_w{}^2 - 4.794 \times 10^{-9} \times T_w{}^3\right] \quad \text{for } T_w < 70°\text{C} \quad (4)$$

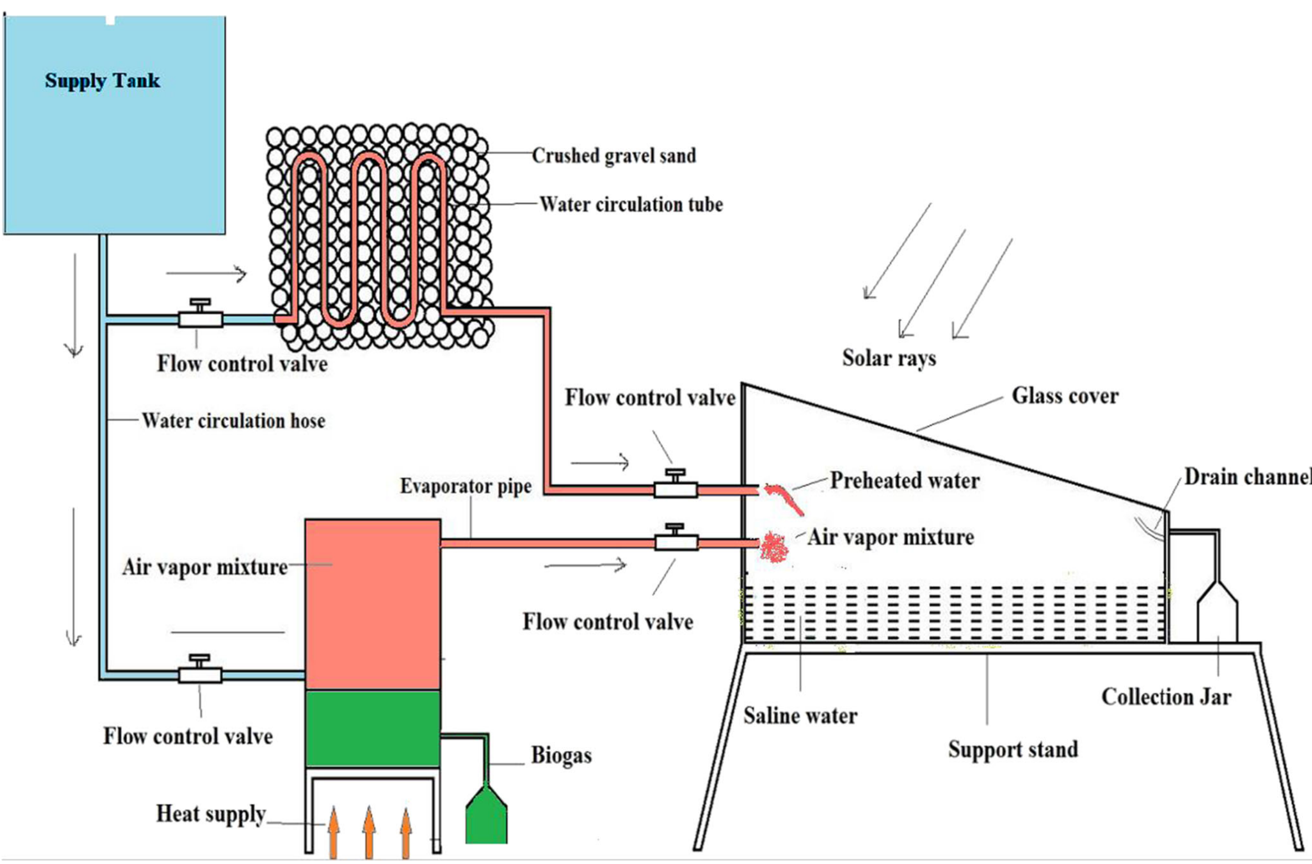

Fig. 1 Schematic view of CGS-BSS

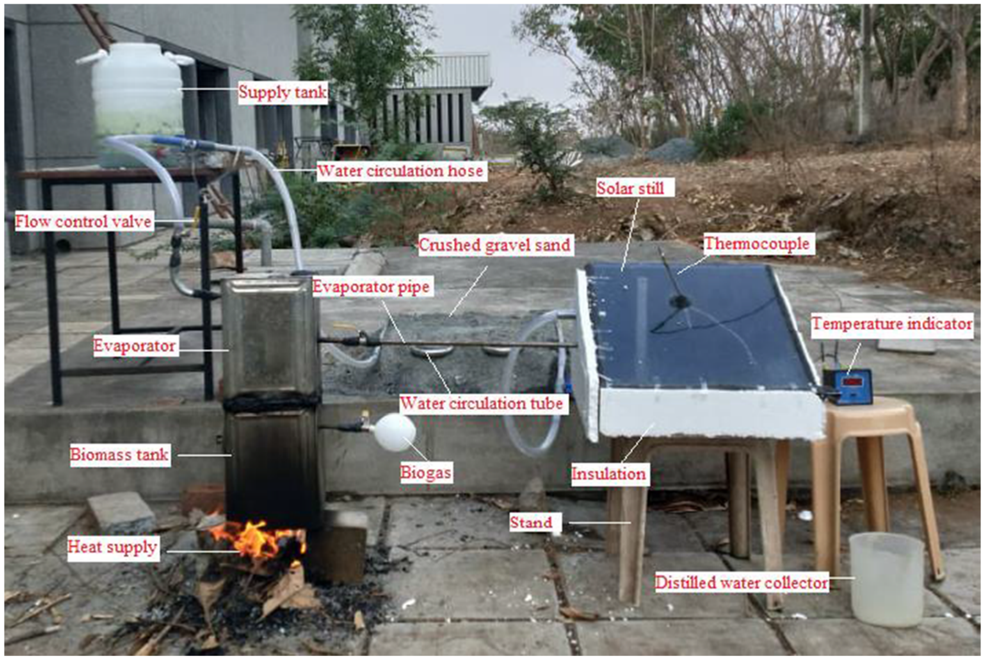

Fig. 2 Photographic view of CGS-BSS

$L = 3.1615 \times (10^6 - 761.6\ T_w)$ for $T_w > 70$ °C (5)

Hourly productivity (Elango et al. 2015):

$$m_w = \frac{h_{eva\ w-g}\left(T_w - T_g\right) \times 3600}{L} \tag{6}$$

Energy efficiency (Elango et al. 2015):

$$\eta_{E,ss} = \frac{m_w \times L}{A_{ss} \times \sum(I_{ss}) \times 3600} \tag{7}$$

Exergy analysis

The required mathematical relations using thermodynamics second law is provided to evaluate the energy losses in solar stills. The following assumptions are made (Dhivagar and Mohanraj 2021c):

- Solar still has steady-state heat transfer processes.

Table 2 Measuring device specification

Instrument	Accuracy	Range	Error (%)
Thermometer	± 0.2 °C	0-100°C	0.5
Thermocouple (K-type)	± 0.1 °C	0–200°C	0.5
Digital temperature indicator	± 0.1 °C	0–200°C	1.2
Solar intensity meter	± 5 W/m^2	0–1000 W/m^2	1.5
Cup type anemometer	± 0.1 m/s	0–15 m/s	10
Measuring jar	± 10 ml	0–1000 ml	10

- Impacts in potential, kinetic, and chemical effects are ignored.
- Saline water temperature is constant at all the locations of basin.

Exergy performance of solar stills is evaluated using the following relations (Hepbasli 2006):

$$Ex_{out} = Ex_{eva} = \frac{\sum m_w \times L \times \left(\frac{T_a + 273}{T_w + 273}\right)}{3600} \tag{8}$$

$$Ex_{in} = Ex_s = A_{ss} \times \sum I_s \times \left[1 - \frac{4}{3} \times \left(\frac{T_a + 273}{T_s}\right) + \frac{1}{3} \times \left(\frac{T_a + 273}{T_s}\right)^4\right] \tag{9}$$

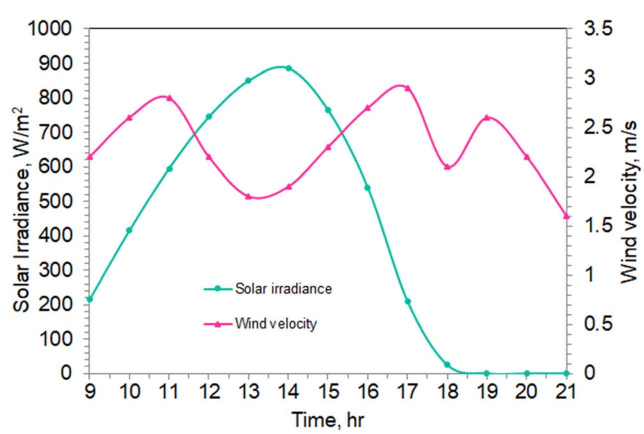

Fig. 3 Variations of solar irradiation and wind velocity

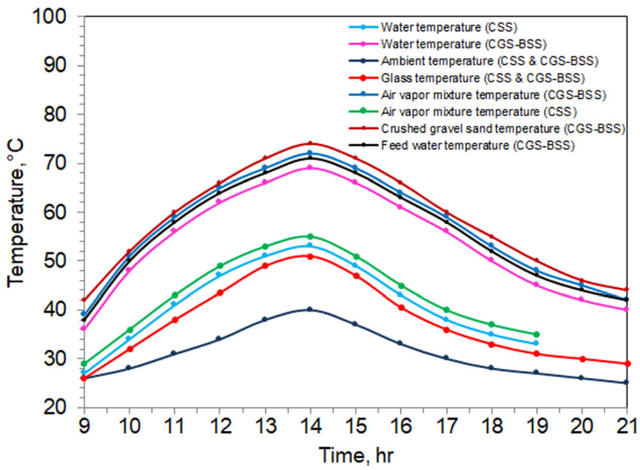

Fig. 4 Variations of different temperatures in CGS-BSS and CSS

Exergy efficiency:

$$\eta_{Ex} = \frac{\sum Ex_{eva}}{\sum Ex_s} \quad (10)$$

Economic analysis

The economic feasibility of solar stills is assessed using the following relations (Esfahani et al. 2011):

$$FAC = CRF \times CC \quad (11)$$

$$CRF = \frac{i(1+i)^n}{(1+i)^n - 1} \quad (12)$$

Here, the interest rate (i) is 12%.

$$ASV = SSF \times S \quad (13)$$

$$S = 0.2 \times CC \quad (14)$$

$$SFF = \frac{i}{(1+i)^n - 1} \quad (15)$$

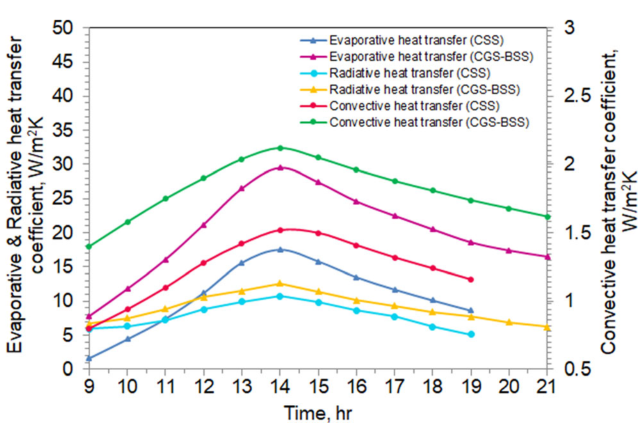

Fig. 5 Variations of evaporative, radiative, and convective heat transfer coefficients

$$AMC = 0.15 \times FAC \quad (16)$$

$$AC = FAC + AMC - ASV \quad (17)$$

$$CPL = \frac{AC}{P_d} \quad (18)$$

$$PBP = \frac{Investments}{Net\ earnings} \quad (19)$$

The annual productivity is observed during clear sunny days (selected 270 days).

Enviro-economic analysis

The CO_2 emissions and CCE by solar stills during its lifetime is estimated using enviro-economic analysis. The CO_2 emissions during combustion of fossil fuels in conventional power plants are estimated as 1.58 kg/kWh (Dwivedi and Tiwari 2012).

CO_2 emissions of the solar still (kg) = $E_{in} \times 1.58$ (20)

Annual energy output is estimated by:

$$E_{out} = \frac{m_w \times L}{3600} \quad (21)$$

Net CO_2 emission (10-year lifetime) is evaluated by:

$$N_{co_2} = \frac{(E_{out} \times LT - E_{in}) \times 1.58}{1000} \quad (22)$$

Carbon credit earned (CCE) is assessed by the following relations:

$$CCE = N_{co_2} \times R_{co_2} \quad (23)$$

Uncertainty analysis

The estimation of uncertainties during the experimentations is given by Holman (2007):

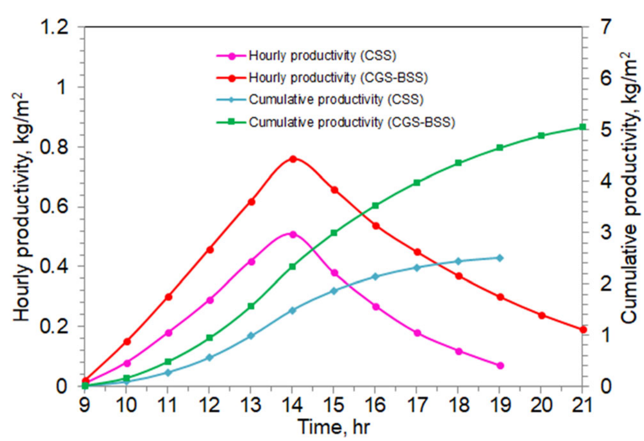

Fig. 6 Variations of hourly and cumulative productivity in CGS-BSS and CSS

$$w_r = \left[\left(\frac{\partial R}{\partial x_1} w_1 \right)^2 + \left(\frac{\partial R}{\partial x_2} w_2 \right)^2 + \ldots\ldots\ldots + \left(\frac{\partial R}{\partial x_n} w_n \right)^2 \right]^{1/2} \quad (24)$$

Here, the function is R, the total uncertainty is w_r, x is called independent variable, and w is also the independent variable with respect to the uncertainty. From the above equation, the uncertainties in temperatures, productivity, energy, and exergy efficiencies are estimated as ± 0.2 °C, ± 5 ml, ± 2.1%, and ± 1.2%, respectively.

Results and discussion

The experimentations have been carried out in both CGS-BSS and CSS during the sunny climatic conditions of 2019. The results observed in CGS-BSS were compared with CSS under the similar climate conditions.

Experimental observation

The variations of solar irradiation and wind velocity are illustrated in Fig. 3. During morning hours, the solar irradiation was gradually increasing and attained the higher value of about 886.1 W/m^2. In between, the formation of clouds was reducing the length of sunshines considerably. Hence, in evening hours, the intensity of solar irradiation was reduced slowly and reached to lower value of about 27.3 W/m^2. The wind velocity is playing the major role during the condensate. However, the observed wind velocity was changing between 1.5 and 2.9 m/s during the experimentation.

The variations of different temperatures in both CGS-BSS and CSS are depicted in Fig. 4. It is noticed that, during afternoon hours (14:00 hours), the observed maximum ambient and glass temperature were about 40.1 °C and 51.6 °C, respectively, and during evening time, it was reduced to about 24.2 °C and 29.8 °C, respectively. It happens due to the intensity of solar irradiation reduces. In addition, the air vapor mixture of CGS-BSS and CSS was increased during 11:00 hours and attained the maximum value of about 71.8 °C and 55.1 °C, respectively. During night time (21:00 hours), it was reduced to about 42.1 °C and 34.3 °C, respectively, in CGS-BSS and CSS. The observed air-vapor mixture temperature of CGS-BSS is 23.2% higher than CSS. The maximum observed temperature of crushed gravel sand and feed water temperature were 74.2°C and 70.6 °C, respectively, in CGS-BSS. Furthermore, during 14:00 hours, the higher saline water temperature in CGS-BSS and CSS were observed by 69.1 °C and 53.2 °C, respectively. It was improved significantly in CGS-BSS due to the impact of preheating technique using crushed gravel sand and hot air vapor from biomass heat source evaporator. The observed saline water temperature in CGS-BSS is 23% higher than the saline water temperature of CSS.

The variations of evaporative, radiative, and convective heat transfer coefficients of CGS-BSS and CSS are depicted in Fig. 5. It is noted that, during afternoon hours, the evaporative heat transfer coefficient observed in both CGS-BSS and CSS were improved by about 29.5 W/m^{2}K and 17.5 W/m^{2}K,

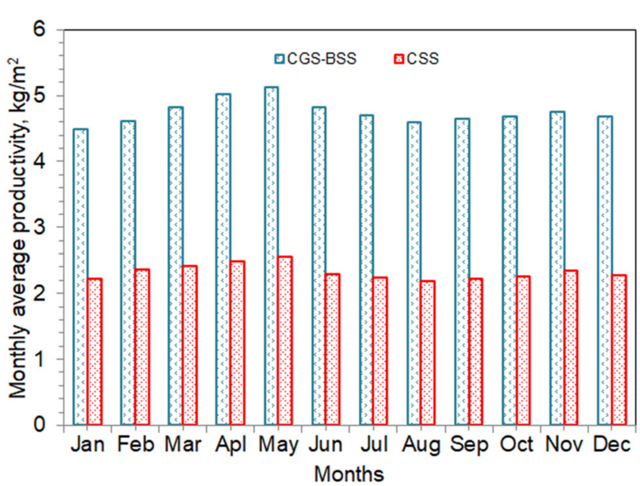

Fig. 7 Monthly average productivity of CGS-BSS and CSS

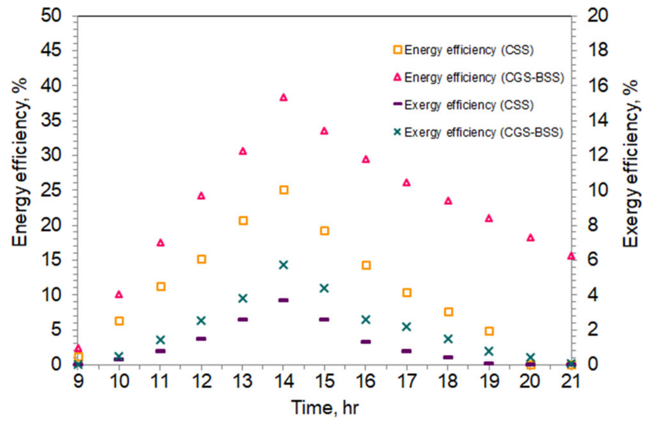

Fig. 8 Variations of energy and exergy efficiencies in CGS-BSS and CSS

Table 3 Economic analysis of CGS-BSS and CSS (1 USD = Rs. 74.25)

Parameters	CGS-BSS	CSS
Capital cost (CC)	Rs. 15139	Rs. 6072
Capital recovery factor (CRF)	0.177	0.177
Fixed annual cost (FAC)	Rs. 2679.5	Rs. 1074
Salvage value (S)	40.78	16.35
Sinking fund factor (SFF)	0.056	0.056
Annual salvage value (ASV)	2.28	0.91
Annual maintenance cost (AMC)	Rs. 401.5	Rs. 201
Annual cost (AC)	Rs. 2912	Rs. 1168
Annual productivity (P_d)	1382.4 kg	675.2 kg
Cost per liter of productivity (CPL)	Rs. 2.10	Rs. 172
Payback period	4.7 months	3.9 months

Table 4 The embodied energy of CGS-BSS and CSS (Piyush et al. 2018)

Solar still components	Embodied energy (E_{in}) CGS-BSS kWh	Embodied energy (E_{in}) CSS kWh
Basin plate	55.5	55.5
Frame body	138.8	138.8
Glass cover	25	25
Insulation	2.7	2.7
Basin plate coating	12.5	12.5
Silicon rubber seal and control valve	6.9	6.9
Crushed gravel sand	15.2	-
Water circulation pipe	83.3	-
Plastic storage tank	22	-
Biomass setup	194.4	-
Evaporator pipe	55.5	-
Total embodied energy	611.8	241.4

respectively. In CGS-BSS, the observed evaporative heat transfer coefficient is 40.6% higher than CSS. This happens due to the preheating technique and the increase of bouncy force at the saline water surface in solar still basin. It also happens due to the inlet hot air vapor through biomass heat source evaporator. The evaporative heat transfer coefficient observed in CGS-BSS is 17.9% higher than the same observed in solar still using magnets (Dumka et al. 2019b). The observed maximum radiative heat transfer coefficient of CGS-BSS and CSS were about 12.6 W/m^2K and 10.7 W/m^2K, respectively. Even though the glass cover temperature was same for both the solar stills, the observed saline water temperature in CGS-BSS was 23% higher than CSS. This results in enhancing the radiative heat transfer rate in CGS-BSS significantly. The radiative heat transfer coefficient of CGS-BSS is 15.07% higher than CSS. Furthermore, the convective heat transfer coefficient of CGS-BSS and CSS was improved by about 2.1 W/m^2K and 1.52 W/m^2K, respectively. During afternoon hours, the convective heat transfer coefficient difference between CGS-BSS and CSS was observed to be about 0.58 W/m^2K. In CGS-BSS, the observed convective heat transfer coefficient is 27.6% higher than CSS. Furthermore, it is 5.9% higher than previous work reported in solar still using magnets heat storage materials (Dumka et al. 2019b).

Productivity

The hourly and cumulative productivity in CGS-BSS and CSS is depicted in Fig. 6. In solar stills, the usage of preheating technique was significantly improving the productivity during high sunshine hours (Dhivagar and Mohanraj 2021d). During morning to afternoon hours (11:00 to 15:00 hours), the hourly productivity of CGS-BSS was significantly improved when compared to CSS. In CGS-BSS, the maximum hourly productivity of about 780 ml was observed during 14:00 hours due to the acceleration in the evaporative heat transfer rate by preheated saline water and hot air vapor. Similarly, during 14:00 hours, the improved productivity of about 510 ml was collected in CSS. In CGS-BSS, the observed maximum productivity is 34.6% higher than CSS. The hourly productivity of CGS-BSS is 16.6% higher than the productivity observed in earlier research work reported using biomass-assisted stepped cup solar still (Chandran et al. 2020). It is noticed that the observed cumulative productivity in CGS-BSS and CSS were about 5.12 kg/m^2 and 2.51 kg/m^2, respectively. The cumulative productivity in CGS-BSS is 50.7 % higher than the productivity collected in CSS. The monthly average productivity for CGS-BSS and CSS is depicted in Fig. 7. Experiments have been conducted for 21 days of clear sunny climatic conditions in a month and

Table 5 Enviro-economic analysis of CSS and CGS-BSS

Solar stills	Annual productivity (kg)	E_{in} (kWh)	E_{out} (kWh)	CO_2 emissions (kg)	Net CO_2 emission (tons)	CCE (Rs)
CSS	675.2	241.4	542.3	381.4	8.18	14576.2
CGS-BSS	1382.4	611.8	1114.2	966.6	16.63	29633.5

considered those average cumulative productivity as monthly average productivity for each month of the year. During summer months (March, April, and May), the higher cumulative productivity was obtained in both the solar stills. It happens due to the more availability of solar irradiation. The observed potential sunshine length during these months was in the range between 8 and 9 h. Moreover, the ambient temperature was varied in the range between 28 and 41 °C. Even though the observation has been made for each month, the maximum results observed during May month is provided for all other performance comparison.

Energy and exergy performance

The experimental observation made on 05.02.2019 was used to evaluate the energy and exergy performances in CGS-BSS and CSS. During this day, the minimum fluctuations were observed in the ambient conditions. The energy and exergy efficiencies of CGS-BSS and CSS are depicted in Fig. 8. It is noticed that, during 14:00 hours, the energy efficiency of CGS-BSS and CSS was improved to 38.3% and 25.1%, respectively. The enhancement in saline water temperature and air-vapor mixture led to the improvement of the energy conversion rate of CGS-BSS significantly. The observed energy efficiency in CGS-BSS is 34.4% higher than CSS. The maximum energy efficiency obtained in CGS-BSS is 16.4% higher than the same observed in previous work done by solar still with humidification and dehumidification concepts (Deniz and Cinar 2016). In exergy efficiency, during morning to afternoon hours, it was improved slowly and reduced considerably at off sunshine hours. The exergy efficiency of CGS-BSS and CSS was significantly improved to about 5.7% and 3.7%, respectively. It is noticed that, the observed exergy efficiency in CGS-BSS is 35% higher than CSS. It happens due to the higher heat release to the atmosphere at higher solar irradiation hours. The maximum exergy efficiency obtained in CGS-BSS is 51.5% higher than the same observed in previous work done by solar collector-assisted solar still (Deniz 2016).

Economic analysis

The cost effectiveness in both CGS-BSS and CSS was estimated using economic analysis and listed in Table 3. The solar still basin and top glass cover are cleaned by weekly basis to prevent the corrosion and dust accumulation. Hence, the capital cost calculated in this experimentation was the combination of fabrication, maintenance and operation costs (Dhivagar and Mohanraj 2021c). In CGS-BSS, it is noticed that CPL of productivity was estimated by Rs. 2.10, which is 94.3% less than the previous work done by biomass-assisted stepped cup solar still (Chandran et al. 2020). In addition, the CPL of CGS-BSS is 18% lower than the CPL estimated in CSS. Furthermore, the PBP of CGS-BSS and CSS was estimated as 4.7 months and 3.9 months, respectively. The observations proved that the increase in annual productivity of solar still decreases the CPL and PBP significantly.

Enviro-economic analysis

The CO_2 emissions of CGS-BSS and CSS were estimated using enviro-economic analysis. Table 4 provides the individual embodied energy in both CGS-BSS and CSS components. These embodied values of each solar still components are differed with respect to the type of materials used for the manufacturing process. The total embodied energy of all the components in CGS-BSS and CSS were estimated as 611.8 kWh and 241.4 kWh, respectively. Table 5 lists the variations in CO_2 emissions and CCE for both the solar stills during the lifetime of 10 years. It is observed that the net CO_2 emission of the CGS-BSS and CSS was estimated as 16.63 tons and 8.18 tons, respectively. The market price of 1 ton of CO_2 emission is estimated as Rs. 1781.93 approximately (Dwivedi and Tiwari 2012). Hence, the CCE for both CGS-BSS and CSS was estimated as Rs. 29633.5 and Rs. 14576.2, respectively. Finally, it is clearly observed that the CCE in CGS-BSS was increased with respect to increase in daily productivity.

Conclusions

The major outcomes observed during the experimentations of both CGS-BSS and CSS are listed below:

a) The air vapor mixture temperature was significantly improved in this preheating technique by crushed gravel sand and biomass evaporator heat source. The CGS-BSS has 23.2% improved air vapor mixture temperature when compared to CSS. The convective and evaporative heat transfer rate observed in CGS-BSS and CSS was 27.6% and 40.6% higher than CSS.
b) The productivity improvement observed in hourly basis of CGS-BSS was 34.6% than the CSS. In addition, the cumulative productivity in CGS-BSS was 50.7% higher than the cumulative productivity observed in CSS. The usage of preheated saline water and hot air vapor enhanced the daily productivity considerably.
c) The observed energy and exergy efficiency of CGS-BSS were improved to about 34.4% and 35% when compared with CSS. The PBP of CGS-BSS and CSS is found to be 4.7 months and 3.9 months, respectively. In enviro-economic analysis, the CO_2 emission of both CGS-BSS and CSS was found to be about 16.63 tons and 8.18 tons, respectively. The CCE in both CGS-BSS and CSS was estimated as Rs. 29633.5 and Rs. 14576.2, respectively.

Appendix

In energy analysis, the mathematical relations of P_g, P_w, and ε_{eff} are given below:

$$P_g = exp\left[25.317 - \frac{5,144}{T_g + 273}\right] \tag{25}$$

$$P_w = exp\left[25.317 - \frac{5,144}{T_w + 273}\right] \tag{26}$$

$$\varepsilon_{eff} = \frac{1}{\left[\frac{1}{\varepsilon_w} + \frac{1}{\varepsilon_g} - 1\right]} \tag{A3}$$

Nomenclature A , basin area, m^2; E , energy, W; E_x, exergy, W; $I(t)$, solar irradiation, W/m^2; h, heat transfer co-efficient, W/m^2K; L, latent heat, kJ/kg; m, hourly productivity, kg; n, number of years; P, pressure, N/m^2; T, temperature, K; N_{co_2} , net CO_2 mitigation; R_{co_2} , market price of CO_2 mitigation

Greek symbol ε_{eff}, effective emissivity; σ, Stefan-Boltzmann constant, 5.67×10^{-8} W/m^2K^4; η, efficiency

Subscripts a, ambient air; c, convection; eva, evaporation; g, glass; in, embodied energy; n, annual rate; o, overall; out, output energy; p_d, annual productivity; s, sun; ss, solar still; w, water

Abbreviations *AC*, annual cost; *AMC*, annual maintenance cost; *ASV*, annual salvage value; *CGS-BSS*, crushed gravel sand and biomass solar still; *CC*, capital cost; *CCE*, carbon credit earned; *CPL*, cost per liter; *CRF*, capital recovery factor; *CSS*, conventional solar still; *FAC*, fixed annual cost; *LT*, life time of the solar still; *PBP*, payback period; *S*, salvage value; *SFF*, sinking fund factor

Acknowledgements The authors would like to thank the anonymous reviewers for their useful comments and suggestions.

Author contribution Ramasamy Dhivagar— Conceptualization, Methodology, Investigation, Writing - original draft.
Murugesan Mohanraj— Supervision.
Yerzhan Belyayev— Supervision.

Availability of data and materials Applicable.

Declarations

Ethical approval Not applicable.

Consent to participate Not applicable.

Consent to publish Not applicable.

Competing interests The authors declare no competing interests.

References

Abdullah AS, Younes MM, Omara ZM, Essa FA (2020) New design of trays solar still with enhanced evaporation methods – comprehensive study. Sol Energy 203:164–174

Bait O (2019) Exergy, environ-economic and economic analyses of tubular solar water heater assisted solar still. J Clean Prod 212:630–646

Belyayev Y, Mohanraj M, Jayaraj S, Kaltayev A (2019) Thermal performance simulation of a heat pump assisted solar desalination system for Kazakhstan conditions. Heat Transf Eng 40:1060–1072

Chandran R, Kandhasamy R, Velan Subramanian C, Veeranan S, Subramaniyan D (2020) Experimental investigation and comparison of desalination using conventional solar still and stepped cup solar still with and without biomass. Therm Sci 24:429–436

Deniz E, Cinar S (2016) Energy, exergy, economic and environmental (4E) analysis of a solar desalination system with humidification-dehumidification. Energy Convers Manag 126:12–19

Deniz E (2016) Energy and exergy analysis of flat plate solar collector–assisted active solar distillation system. Desal Wat Treat 57:13–21

Dhivagar R, Sundararaj S (2018) A review on methods of productivity improvement in solar desalination. Appl Mech Mater 877:414–429

Dhivagar R, Sundararaj S (2019) Thermodynamic and water analysis on augmentation of a solar still with copper tube heat exchange in coarse aggregate. J Therm Anal Calorim 136:89–99

Dhivagar R, Mohanraj M, Hidouri K, Belyayev Y (2020) Energy, exergy, economic and enviro-economic (4E) analysis of gravel coarse aggregate sensible heat storage-assisted single-slope solar still. J Therm Anal Calorim 145:475–494

Dhivagar R, Mohanraj M, Hidouri K, Midhun M (2021a) CFD modeling of a gravel coarse aggregate sensible heat storage assisted single slope solar still. Desal Wat Treat 210:54–69

Dhivagar R, Mohanraj M, Praveen Raj, Radha Krishna G (2021b) Thermodynamic analysis of single slope solar still using graphite plates and block magnets at seasonal climatic conditions. Water Sci Technol. In press.

Dhivagar R, Mohanraj M (2021c) Performance improvements of single slope solar still using graphite plate fins and magnets. Environ Sci Pollut Res 28:20499–20516

Dhivagar R, Mohanraj M (2021d) Optimization of performance of coarse aggregate-assisted single-slope solar still via Taguchi Approach. J Renew Energy Environ 8:13–19

Dumka P, Sharma A, Kushwah Y, Raghav AS, Mishra DR (2019a) Performance evaluation of single slope solar still augmented with sand filled cotton bags. J Energy Storage 25:100888

Dumka P, Kushwah Y, Sharma A, Mishra DR (2019b) Comparative analysis and experimental evaluation of single slope solar still augmented with permanent magnets and conventional solar still. Desalination 459:34–45

Dubey M, Mishra DR (2020) Thermo-exergo-economic analysis of double slope solar still augmented with ferrite ring magnets and GI sheet. Desal Wat Treat 198:19–30

Dwivedi VK, Tiwari GN (2012) Thermal modeling and carbon credit earned of a double slope passive solar still. Desal Wat Treat 13: 400–410

Elango C, Gunasekaran N, Sampathkumar K (2015) Thermal models of solar still—a comprehensive review. Renew Sust Energ Rev 47: 856–911

Esfahani JA, Rahbar N, Lavvaf M (2011) Utilization of thermoelectric cooling in a portable active solar still – an experimental study on winter days. Desalination 269:198–205

Hassan H (2019) Comparing the performance of passive and active double and single slope solar stills incorporated with parabolic trough collector via energy, exergy and productivity. Renew Energy 148: 437–450

Hepbasli A (2006) A key review on exergetic analysis and assessment of renewable energy resources for a sustainable future. Renew Sust Energ Rev 12:593–661

Holman J.P (2007) Experimental methods for engineers. Tata Mcgraw Hill Publishing Company.

Kabeel AE, Mohamed A, Mahgoub M (2016) The performance of a modified solar still using hot air injection and PCM. Desalination 379:102–107

Modi KV, Modi GJ (2019) Performance of single slope double basin solar stills with small pile of wick materials. Appl Therm Eng 149: 723–730

Omara ZM, El Tawil MA, El Nashar EA (2013) A new hybrid desalination system using wicks/solar still and evacuated solar water heater. Desalination 325:56–69

Omara AAM, Abuelnuor AAA, Mohammed HA, Khiadani M (2020) Phase change materials (PCMs) for improving solar still productivity: a review. J Therm Anal Calorim 139:1585–1617

Piyush P, Rahul D, Dhananjay S, Amimul A (2018) Energy matrices, exergo-economic and enviro-economic analysis of modified multi-wick basin type double slope solar still. Desalination 447:55–73

Rabhi K, Nciri R, Nasri F, Ali C, Bacha HB (2017) Experimental performance analysis of a modified single basin single slope solar still with pin-fins absorber and condenser. Desalination 416:86–93

Sakthivel TG, Arjunan TV (2019) Thermodynamic performance comparison of single slope solar stills with and without cotton cloth energy storage medium. J Therm Anal Calorim 137:351–360

Senthil Rajan A, Raja K, Marimuthu P (2014) Multi basin desalination using biomass heat source and analytical validation using RSM. Energy Convers Manag 87:359–366

Sharon H, Reddy KS, Krithika D, Philip L (2017) Experimental performance investigation of titled solar still with basin and wick for distillate quality and enviro-economic aspects. Desalination 410:30–54

Sharshir SW, Peng G, El Sheikh AH, Edreis EMA, El Tawil MA, Abdelhamid T, Kabeel AE, Zang J, Yang N (2018) Energy and exergy analysis of solar stills with micro/nano particles: a comparative study. Energy Convers Manag 177:363–375